American Mineralogist, Volume 82, pages 69–78, 1997

Montmorillonite under high H_2O pressures: Stability of hydrate phases, rehydration hysteresis, and the effect of interlayer cations

TZY-CHUNG WU,[1,*] WILLIAM A. BASSETT,[1] WUU-LIANG HUANG,[2] STEPHEN GUGGENHEIM,[3] AND AUGUST F. KOSTER VAN GROOS[3]

[1]Mineral Physics Laboratory, Department of Geological Sciences, Snee Hall, Cornell University, Ithaca, New York 14853, U.S.A.
[2]Exxon Production Research Company, Houston, Texas 77252-2189, U.S.A.
[3]Department of Geological Sciences, University of Illinois at Chicago, Chicago, Illinois 60680, U.S.A.

ABSTRACT

Dehydration of Ca- and Mg-exchanged montmorillonite was studied along H_2O isochores in the hydrothermal diamond-anvil cell by in situ X-ray diffraction using a synchrotron radiation source. At pressures between the H_2O liquid-vapor (L-V) boundary and ~10 kbar, the dehydration temperature for the conversion from the 19 Å hydration state to the 15 Å hydration state occurred over the temperature range 260–350 °C for Ca-exchanged montmorillonite and 200–250 °C for Mg-exchanged montmorillonite, with a slight increase with increasing pressure. For both materials, the rehydration from the 15 Å to 19 Å states occurred at the same temperature as dehydration at pressures along the H_2O L-V boundary, thus showing no hysteresis. The rehydration hysteresis increased to nearly 75 °C at 6 kbar for Ca-exchanged montmorillonite and to the same amount at 2.5 kbar for Mg-exchanged montmorillonite. Dehydration experiments on Mg-exchanged montmorillonite along the isochores of 1.024 and 0.75 g/cm^3 showed conversion from the 15 Å hydrate to the 12.5 Å hydrate at 590–605 °C. The 12.5 Å hydrate only partially rehydrated after cooling to room temperature along those two isochores. In an experiment started from the 15 Å state, in which the pressure was below the H_2O L-V curve, dehydration occurred at 400–500 °C and rehydration at 430–350 °C. When our previous results on Na-exchanged montmorillonite are combined with the current experimental data, systematic trends can be found in the effect of pressure and interlayer-cation species on the dehydration temperature and rehydration hysteresis.

INTRODUCTION

The interlayer in montmorillonite is composed of hydrated cations. Because of the low charge of silicate layers (<0.6 unit charge per one-half unit cell), montmorillonite readily hydrates and has a large swelling capability.

For divalent interlayer cations, at a pressure of 1 atm, many previous studies (e.g., McEwan and Wilson 1980) show three discrete hydration states with (001) layer spacings at ~12.5, ~15, and ~19 Å, depending on the H_2O activity in the system. Although those states have been called one-, two-, and three-layer hydrates, respectively, those terms do not accurately represent the real interlayer structures. The configuration of interlayer H_2O depends greatly on the cation size, charge, and charge distribution within the silicate layers (e.g., Clementz et al. 1973; McBride et al. 1975). Therefore, we simply refer to them as the 12.5 Å, 15 Å, and 19 Å hydration states or as the first, second, and third hydration states.

The dehydration of the interlayer is of special interest to geologists because dehydration processes influence pore pressure in rocks, affect rock strength, and contribute to subsurface fluid migration. Evolved water may also be subducted along with the lithospheric plates to the upper mantle. Thus, understanding the effects of temperature, pressure, and other variables on the dehydration reaction in montmorillonite, which is abundant in sedimentary settings, is of considerable importance.

Because of experimental limitations, most earlier studies concentrated on the pressure dependence of smectite dehydration temperature at lower pressures, in which hydrated smectite dehydrates to H_2O in gas phase or in supercritical vapor phase plus dehydrated smectite. Although the earlier data cannot be applied directly to geologic *P-T* conditions, they are valuable because they provide insight into dehydration phenomena and can be compared in part to our data. Stone and Rowland (1955) first studied the pressure dependence of the dehydration temperature in a Ca-rich montmorillonite using differential thermal analysis (DTA) between 1 and 6 bars H_2O pressure. They showed that the temperature for dehydration of the second hydration state to the first hydration state increased from 150 °C at 1 bar to 240 °C at 6 bars. For dehydration from the first hydration state to the an-

* Present address: Applied-Komatsu Technology, 3101 Scott Blvd., M/S 9156, Santa Clara, California 95052, U.S.A.

0003-004X/97/0102-0069$05.00

hydrous state (no H_2O), the temperature increased from 250 °C at 1 bar to 328 °C at 6 bars. Koster van Groos and Guggenheim (1984, 1986, 1987) conducted a series of DTA studies on Na-, K-, Mg-, and Ca-exchanged montmorillonite starting from the second hydration state up to 1.5 kbar. They showed clearly that the dehydration temperature increased steeply at low pressures (<100 bars), and the pressure dependence became much smaller at higher pressures (>480 bars). At 480 bars, the temperatures for dehydration from the second to the first hydration state were found to be 495 and 455 °C for Ca- and Mg-exchanged montmorillonite, respectively. Note that their slope of dehydration boundary gradually changes as the expelled H_2O gradually changes from steam to supercritical vapor with increasing temperature.

Huang et al. (1994) studied the dehydration and rehydration of Na-exchanged montmorillonite along the 0.80 g/cm³ isochore of H_2O in a hydrothermal diamond cell (HDAC) by in situ X-ray diffraction using a synchrotron radiation source. This was the first experimental study in which a pure smectite sample was subjected to *P-T* conditions comparable to those found in geologic situations, where hydrated smectite would dehydrate to liquid water plus dehydrated smectite. They found that along the 0.80 g/cm³ isochore of H_2O, the third hydration state was stable up to 330 °C at a pressure near 1450 bars. After completion of the conversion to the 15 Å hydrate at 385 °C, subsequent cooling did not result in rehydration of montmorillonite until the temperature dropped below 200 °C. Near room temperature, it partially rehydrated back to ~17.75 Å.

Here we report the results from a more extensive study of the dehydration-rehydration behaviors of Ca- and Mg-exchanged montmorillonite under high H_2O pressures. Improved techniques have made it possible for us to investigate these species in greater detail and over a wider *P-T* range, including those found in geologic settings. In addition to measuring the pressure dependence of dehydration temperature, we observed the effects of pressure on rehydration and dehydration-rehydration hysteresis. We also evaluated the effect of ionic potential of interlayer cations on dehydration behavior.

Experimental methods and procedures

Ca- and Mg-exchanged montmorillonite samples, Clay Mineral Society Source Clay SWy-1 (Wyoming bentonite), were used as starting material. Details of sample preparation, X-ray diffraction, and chemical data were given by Koster van Groos and Guggenheim (1987). Only the hydraulic fraction of <0.1 μm was used, and cation exchange was accomplished by four washings with 1*N* solution of $CaCl_2$ or $MgCl_2$ followed by six washings with distilled water and drying in air. The samples are henceforth referred to as CaSWy-1 and MgSWy-1. The samples were stored at 55% humidity over a saturated solution of $Mg(NO_3)_2 \cdot 6H_2O$ until they were sent to Cornell University. At 55% relative humidity, the samples were in the second hydration state. X-ray data of the starting material before the hydrothermal experiments confirmed that the samples remained in the second hydration state. When distilled-deionized water was added to the sample chamber of the HDAC, the sample converted to the third hydration state, or the 19 Å phase.

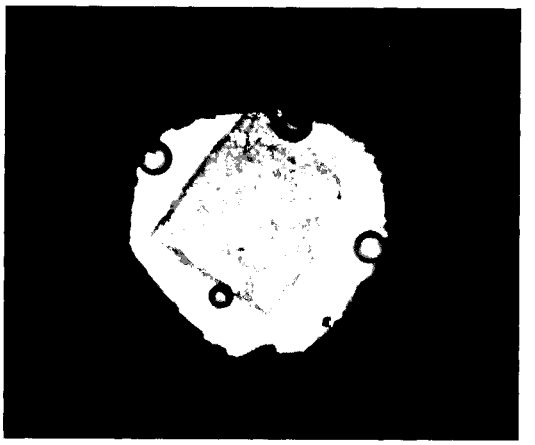

Figure 1. Photomicrograph of a typical Ca-exchanged montmorillonite sample in a sample chamber with water and air bubbles. The sample is square because it was cut with a razor blade. The density of water after homogenization of this sample was ~0.88 g/cm³. The sample chamber is ~500 μm across. The samples looked very similar before and after a run; therefore, it is concluded that they remained intact throughout heating and cooling. The bubble before and after a run usually showed a negligible change in size, indicating that the isochore density remained within fairly narrow limits.

The HDAC (Bassett et al. 1993) has two resistance heaters around the upper and lower diamond seats and two thermocouples attached to both diamond anvils to measure their temperatures. The sample and water are loaded into the sample chamber, a 500 μm diameter hole in a 125 μm thick rhenium foil (Fig. 1). The sample chamber is quickly sealed by lowering the upper diamond anvil. During the loading, an air bubble is usually trapped in the chamber. The ratio of the volume of air bubble to that of water determines the density of the fluid after homogenization. The isochoric density of the fluid must be known to determine the pressure from the measured temperature. If the density of the fluid is <1 g/cm³ (bubbles occurred at loading), homogenization temperature, T_h, is used to determine the density on the basis of the *PTV* relationship of H_2O (Wagner and Pruss 1993). If the density of the fluid is >1 g/cm³ (no bubble observed), the density is determined from therelationship of the pressure vs. ice-melting temperature (T_m) (Wagner et al. 1994). For a known fluid density the pressure is calculated from the temperature (assuming the volume of the sample chamber is constant) using the equation of state of water (Saul and Wagner 1989).

Laser interferometry was used to monitor the dimensions of the sample chamber during heating. The change in volume was about 1% during heating and <0.5% during cooling. T_h was measured before and after each run,

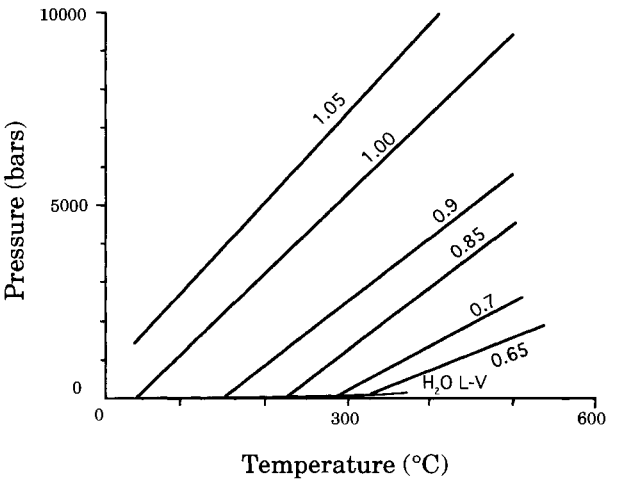

FIGURE 2. *P-T* diagram showing the isochores of the heating paths followed during experiments. Numbers next to each line represent the densities of the H_2O isochores in grams per cubic centimeter.

to determine the heating and cooling paths, and the appropriate uncertainty was determined.

Real-time energy-dispersive X-ray diffraction (EDXRD) was used to analyze samples at high pressure and temperature at the B-1 station of the Cornell High Energy Synchrotron Source (CHESS). The 2θ diffraction angle used for all runs was 3°, and the $E \cdot d$ (the product of energy and the d value) factor for calculating d values was calibrated with gold and the 001 peak of kaolinite before or after a series of runs. Average accumulation time for a diffraction pattern was 1–2 min.

Specimens of both Ca- or Mg-exchanged montmorillonite were observed to remain intact during heating and cooling cycles. The specimens became opaque during dehydration and transparent again during rehydration. For greater detail regarding temperature calibration, pressure determination, and other experimental details, the reader is referred to Wu et al. (1995).

RESULTS

Ca-exchanged montmorillonite

Eight high-temperature closed-cell experiments were made on CaSWy-1, with more than 500 X-ray diffraction patterns taken along heating and cooling paths. The isochoric pressure-temperature paths are plotted in Figure 2.

Except for experiments at starting pressures >1 bar, CaSWy-1 was in an initial hydration state with a d value of 19.05 Å. EDXRD patterns recorded for a dehydration-rehydration cycle along the 1.053 g/cm³ isochore are shown in Figure 3. Because of the high degree of ordering perpendicular to the c axis, the 020 peak is readily observed. Note that the room-temperature pattern shows some sample without interlayer H_2O (d = 9.6 Å). The intensity of this peak becomes very weak at 150 °C.

Of the eight runs, six were complete heating-cooling

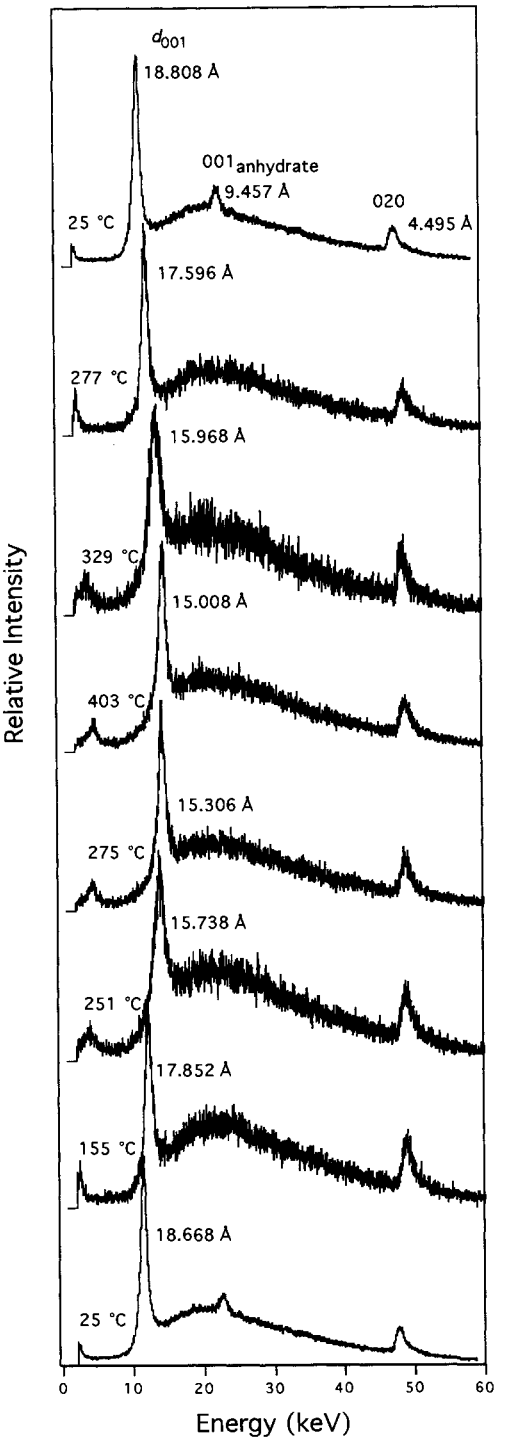

FIGURE 3. Series of energy-dispersive X-ray diffraction patterns of CaSWy-1 during a heating-cooling cycle with isochoric density of 1.053 g/cm³, showing the dehydration process starting at the top and the rehydration process ending at the bottom.

TABLE 1. Summary of hydrothermal experiments on various cation-exchanged SWy-1 montmorillonite samples

Sample-run	ρ_{fluid} (g/cm³)	H_2O^i	T_{DH} (°C)	P_{DH} (bar)	T_{RH} (°C)	P_{RH} (bar)	H_2O^f	Comments
Ca1107-1	1.048	3	300–350	7075–8265	270–190	6340–4420	3	
Ca1107-2	1.053	3	300–350	7550–8555	265–175	6415–4280	3	
Ca1107-3	0.877	3	275–340	1450–2510	300–265	1880–1270	3	
Ca1107-4	0.895	3	275–350	1750–3060	300–260	2130–1450	3	
Ca1106-1	0.704	3	260–310	48–150	300–255	82–43	3	
Ca1106-2	0.720	3	260–310	48–260	300–260	160–48	3	
Ca1111	0.625	3	260–310	48–96	n.a.	n.a.	3	Heating along L-V curve
Ca1111b	<0.017	2	240–270	~22	n.a.	n.a.	n.a.	
Mg323-1	0.9–1.0	3	200–245	550–1330	170–140	2340–1740	3	
Mg323-2	1.024	3	a. 215–250	a. 4106–4891				RH was from 1 to 2 layers
			b. 600–605	b. 12670–12780	50	905	2 + 1	
Mg326-1	0.75	3	200–245	16–37	245–200	19–16	3	Heating along L-V curve
Mg326-2	0.75	3	a. 200–240	a. 16–33				RH was from 1 to 2 layers
			b. 590–600	b. 3740–3860	150	5	2 + 1	
Mg319	<0.1	2	400–500	<199–271	430–350	<159–122	2	
Na921-1	0.80	3	330–385	1468–2309	200–40	15–1	3	
Na921-2	0.80	3	a. 330–385	a. 1468–2309	n.a.	n.a	n.a.	
			b. 485–500	b. 4400–4550				

Note: Letters "a" and "b" in columns T_{DH} and P_{DH} denote the first (19 Å to 15 Å) and second (15 Å to 12.5 Å) dehydration observed, respectively. Data of NaSWy-1 (Na921) are from Huang et al. (1994). ρ_{fluid} = density of fluid; H_2O^i = number of H_2O layers in the initial hydration state: 1 = 12.5 Å, 2 = 15 Å, 3 = 19 Å; T_{DH} = dehydration temperature; P_{DH} = dehydration pressure; T_{RH} = rehydration temperature; P_{RH} = rehydration pressure; H_2O^f = number of H_2O layers in the final hydration state: 1 = 12.5 Å, 2 = 15 Å, 3 = 19 Å.

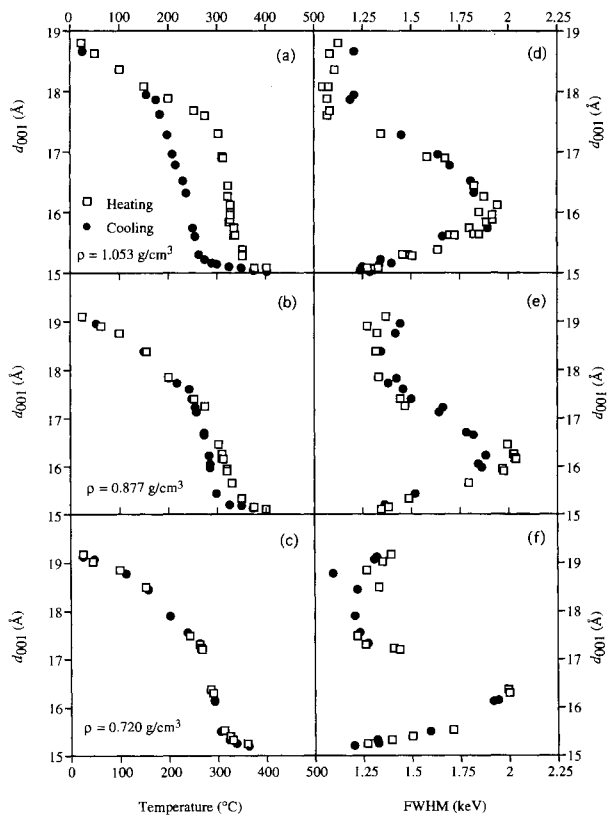

FIGURE 4. The d_{001} values of CaSWy-1 vs. temperature (**a–c**) and the full-width at half-maximum (FWHM) (**d–f**) of the 001 peak. The H_2O isochoric densities are shown.

cycles, which allowed the studies of dehydration-rehydration hysteresis. Those six isochoric paths are divided into three groups on the basis of densities, i.e., densities near 0.7, 0.9, and 1.05 g/cm³ (Table 1). With each change in temperature and pressure, sufficient time was allowed for observed changes in diffraction peaks to proceed to completion. The change of basal d_{001} values vs. temperature along the heating-cooling paths during dehydration-rehydration cycles showed very good agreement between the two experiments for each density group. Figure 4 shows the d_{001} values vs. temperature for three isochores, one from each density group. In Figure 4, it is clear that the d_{001} value gradually decreases from ~19 to ~17.5 Å before rapid dehydration begins in every isochoric heating path. The temperature range for dehydration varies a little between isochores. The ranges are 300–350 °C along ~1.05 g/cm³ isochores, 275–340 °C along ~0.9 g/cm³ isochores, and 260–310 °C for ~0.7 g/cm³ isochores and along the H_2O L-V curve. Those dehydration temperatures and corresponding pressures are summarized in Table 1.

The variation of basal d values with temperature during the rehydration followed the same paths as dehydration along isochores with low H_2O densities, ~0.7 g/cm³ (Fig. 4c). Along isochores with higher H_2O densities, the rehydration occurred at a lower temperature than the dehydration (Figs. 4a and 4b). This rehydration hysteresis clearly increases with increasing pressure.

In Figures 4d–4f, basal d values are plotted against the peak width, defined as the full-width at half-maximum (FWHM). The FWHM evolution along each dehydration and rehydration cycle, determined by Gaussian peak fitting, shows a perfect correlation with the d value regardless of the hysteresis effect.

Two more runs were made along H_2O isochores with

lower densities. Because the hysteresis effect is zero along isochores with densities <0.72 g/cm³, X-ray patterns were taken only on the heating paths in the low-density runs. These data were used to constrain the dehydration-temperature at lower pressures. One run was along the isochore of 0.625 g/cm³. The dehydration-temperature range of the 0.625 g/cm³ isochore was identical to those of 0.704 and 0.720 g/cm³, which was expected because the *P-T* conditions for those isochores were mostly on the H_2O L-V curve when the dehydration occurred.

The other run at very low H_2O density started with soaking the sample in water at 1 atm and room temperature in the sample chamber followed by a leak of water. Only a tiny amount of H_2O was left in the chamber when the chamber was sealed. The H_2O homogenized to the vapor field on heating. T_h was not measured because of the difficulty in determining the last vaporization. The third hydration state dehydrates to the second hydration state at 240–255 °C. This low dehydration temperature implies H_2O homogenized to the vapor phase at <240 °C, causing the heating path to deviate from the H_2O L-V curve. This constrained the density of H_2O in the sample chamber to <0.017 g/cm³.

Mg-exchanged montmorillonite

Five isochoric runs were made on MgSWy-1. Four runs started with the 19 Å hydration state; the other low-density run started with the 15 Å hydration state. The dehydration-temperature ranges measured for the 19 Å to 15 Å transition were 215–250, 200–245, and 200–245 °C for isochoric densities of 1.024, 0.95, and 0.75 g/cm³, respectively (Table 1).

The dehydration-rehydration cycle between the 19 Å and 15 Å hydration states was measured along the 0.95 and 0.75 g/cm³ isochores. The basal spacing is plotted against both temperature and the peak width in Figure 5. The rehydration hysteresis increases from nearly zero along the 0.75 g/cm³ isochore to about 50 °C along the 0.95 g/cm³ H_2O isochore. Although the absolute peak width for the run following the 0.95 g/cm³ isochore is somewhat different during dehydration and rehydration, the maximum peak width does occur at approximately the same basal spacing.

The dehydration-temperature ranges for the 15 Å to 12.5 Å conversion were measured along three heating paths (Fig. 6). They were 600–605 °C along the 1.024 g/cm³ isochore, 590–600 °C along the 0.75 g/cm³ isochore, and 400–500 °C for the low-density run in the vapor field of H_2O (Table 1). The first two runs were continuous for the 19 Å to 15 Å dehydration (Figs. 6a and 6b). The lower density run started from the 15 Å state at room temperature without much saturated H_2O in the sample chamber.

The 12.5 Å to 15 Å rehydration started at ~150 °C for the 0.75 g/cm³ isochore and ~50 °C for the 1.024 g/cm³ isochore, showing hysteresis of ~450 °C for the former and ~550 °C for the latter. The final products for those two runs show two 001 peaks, representing a mixture of 12.5 Å and 15 Å hydrates and implying the rehydration was not complete.

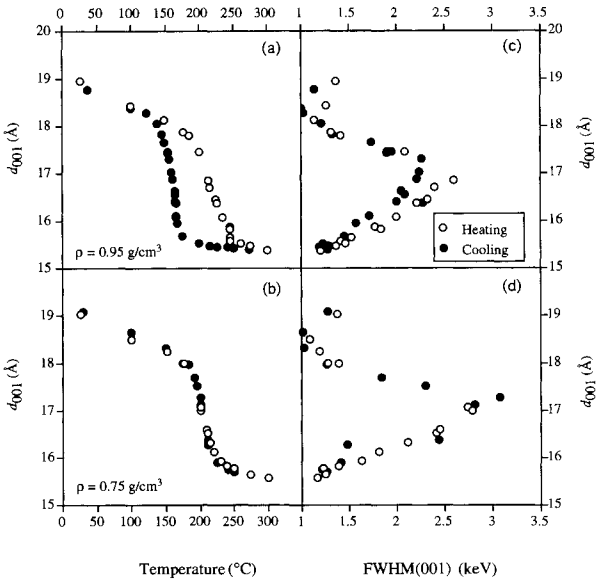

FIGURE 5. The d_{001} values of MgSWy-1 vs. temperature (**a** and **b**) and 001 peak width (**c** and **d**) for the 19 Å to 15 Å dehydration-rehydration cycles along the 0.95 and 0.75 g/cm³ isochores.

The low-density run started with a small amount of saturated water (volume ratio <10 %) at 1 atm and room temperature with a sample in the 15 Å state. The H_2O homogenized to the vapor phase with a density estimated to be <0.10 g/cm³. The dehydration to the 12.5 Å state was completed at 500 °C. During cooling, the rehydration started at about 430 °C and finished by 350 °C, showing a rehydration hysteresis of 80 °C. The lower dehydration temperature and smaller rehydration hysteresis in this lower density run confirmed that the trend of pressure dependence in the 15 Å to 12.5 Å dehydration-rehydration cycle is the same as the trend observed for the 19 Å to 15 Å cycle.

DISCUSSION

Pressure dependence of dehydration temperature

For each isochore, the starting and ending points of dehydration and rehydration occur where the slope abruptly changes in the d_{001} vs. temperature curve (Figs. 4–6). Because the peak broadening, or the variation of FWHM, was independent of the rehydration hysteresis, it can be used as a good indication of transition progress during dehydration and rehydration. For the 19 Å to 15 Å cycle, the middle points of the dehydration and rehydration are defined as the temperature at which the maximum FWHM occurs (Figs. 4 and 5).

Figure 7 shows the CaSWy-1 data plotted in a *P-T* diagram. The distance between the solid line connecting

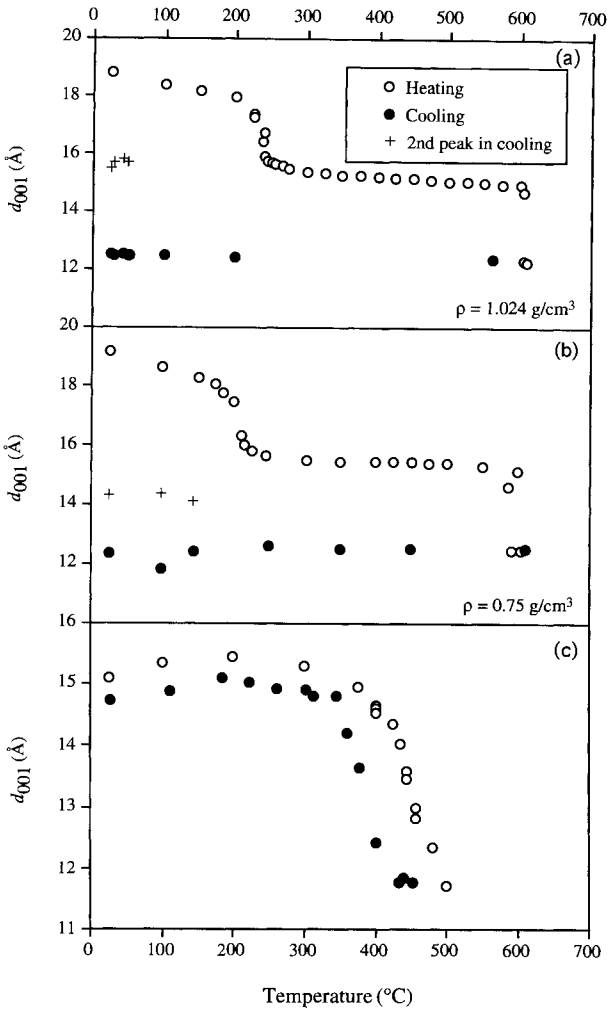

FIGURE 6. The d_{001} values of MgSWy-1 vs. temperature for the dehydration from the 19 Å to 15 Å hydration states and from the 15 Å to 12.5 Å hydration states along the 1.024 g/cm³ and 0.75 g/cm³ isochores in **a** and **b**, respectively. Diagrams **a** and **b** also show partial rehydration at very low temperature, indicated by the appearance of the second 001 peak at ~15 Å (the plus sign). In **c** the clay started from the 15 Å hydrate. The 15 Å to 12.5 Å conversion was observed during heating and cooling at pressures below the H_2O L-V curve, i.e., in the vapor field.

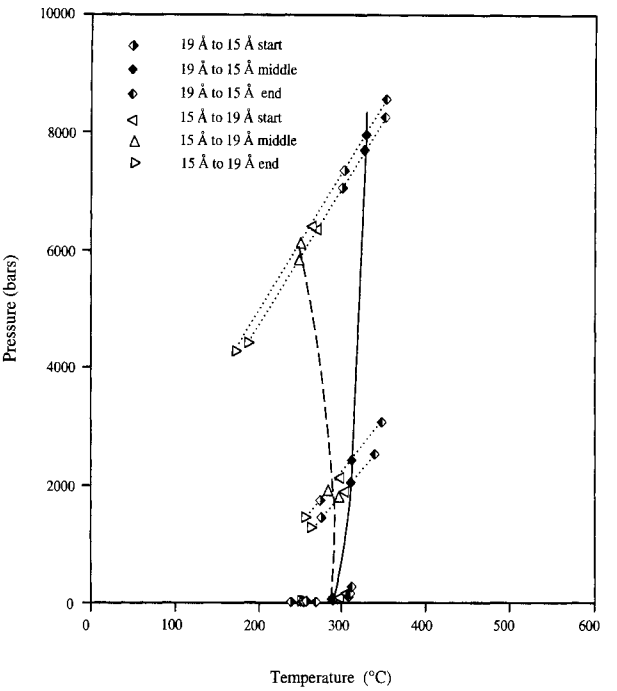

FIGURE 7. *P-T* diagram of CaSWy-1 summarizes the *P-T* conditions for the starting, middle, and ending points of dehydration and rehydration cycles for 19 Å and 15 Å hydrates. The solid line is a visual fit to midpoints of the dehydration process. The dashed line is a visual fit to midpoints of the rehydration process. The distance between the lines indicates the size of rehydration hysteresis. Points collected along the same isochores are connected with dotted lines.

middle points of dehydration and the dashed line connecting those of rehydration defines the magnitude of hysteresis. The dehydration data below 2.5 kbar are plotted in Figure 8. The DTA data of Koster van Groos and Guggenheim (1987), for which the starting basal spacing was 15 Å, can be compared to our low-density data below the H_2O L-V curve. The 50% dehydration contour for the smectite in sedimentary basins predicted by the thermodynamic modeling of Ransom and Helgeson (1995) is also plotted in Figure 8.

Figure 9a shows the MgSWy-1 dehydration-rehydration data of the 19 Å and 15 Å states in a *P-T* diagram. The symbols are the same as those in Figure 7. The dehydration and rehydration data of the 15 Å and 12.5 Å states are plotted in Figure 9b, along with the DTA data of Koster van Groos and Guggenheim (1987) obtained at lower pressures.

Although we collected data along only one isochore below the L-V curve for each material (Figs. 8 and 9b), these show that the dP/dT value of the dehydration curve is much smaller below the L-V curve than above it. Thus, the dehydration temperature increases rapidly with pressure below the L-V curve and slowly with pressure above the L-V curve. According to the Clapeyron equation, the steep, nearly straight dP/dT slope of the dehydration boundary at pressures above the L-V curve probably indicates a small change of volume (ΔV) of H_2O between interlayer and external H_2O. This is in agreement with the Monte Carlo calculations of Chang et al. (1995). The shallow, nearly flat dP/dT slope at pressures below the L-V curve, in contrast, probably results from the large ΔV between the interlayer H_2O and external H_2O vapor. This general trend is a common phenomenon in dehydration reactions of hydrous minerals and is in agreement with the data of previous studies in Ca- and Mg-montmorillonite (Koster van Groos and Guggenheim 1987; Stone and Rowland 1955) at lower pressures.

The data of Koster van Groos and Guggenheim (1987)

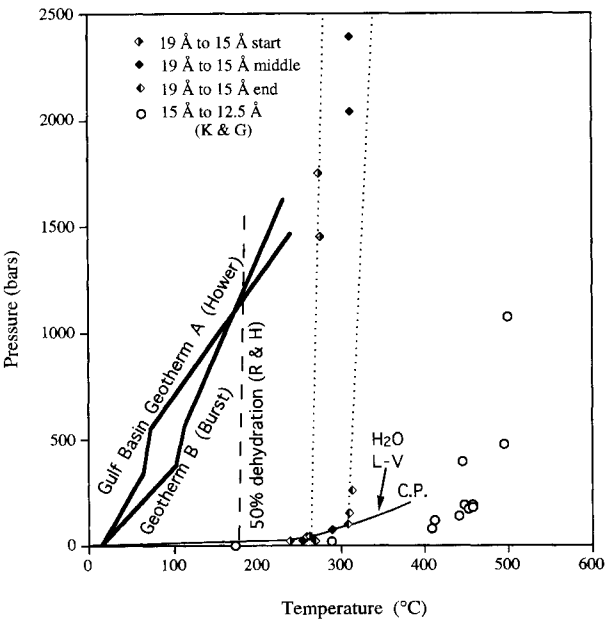

FIGURE 8. *P-T* diagram of CaSWy-1 showing the data of the 19 Å to 15 Å dehydration under a pressure of 2500 bars. The data are compared with the 15 Å to 12.5 Å dehydration data of Koster van Groos and Guggenheim (1987; K & G), shown as open circles, and the results from thermodynamic modeling by Ransom and Helgeson (1995; R & H). The dashed line represents the 50% dehydration contour predicted by the modeling starting from the 15 Å state. The two thick solid lines are two versions of geotherms of the Tertiary sedimentary basin in the U.S. Gulf Coast (Hower et al. 1976; Burst 1969). The H_2O liquid-vapor equilibrium curve is shown as the thin solid line. The dotted lines define the start and completion of dehydration with increasing temperature.

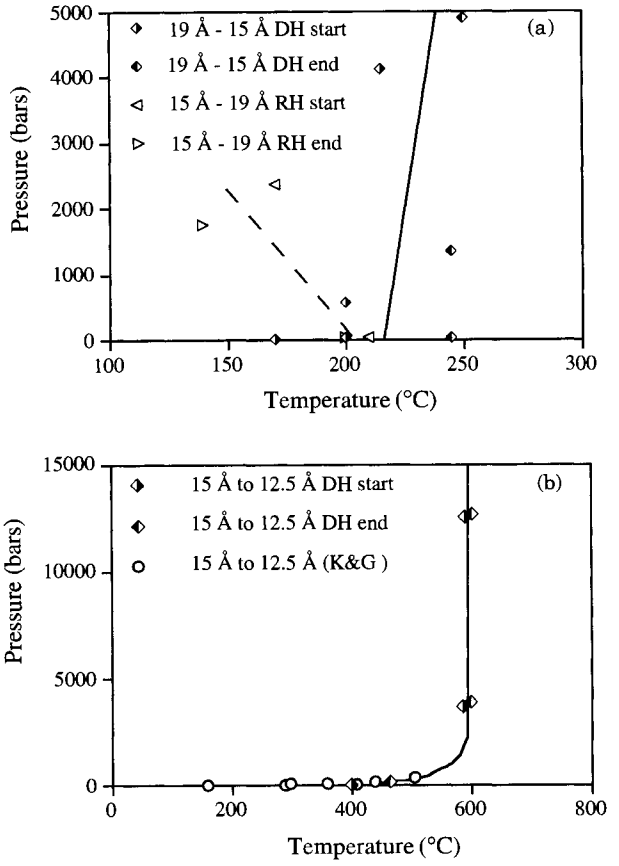

FIGURE 9. *P-T* diagrams of MgSWy-1 showing (**a**) dehydration (DH) and rehydration (RH) data between 19 Å and 15 Å hydrates and (**b**) dehydration data for 15 Å to 12.5 Å hydrates. Our dehydration data are shown as diamonds, and those of Koster van Groos and Guggenheim (1987) are shown as open circles.

for the 15 Å to 12.5 Å dehydration in Figure 8 show a much gentler change in the dP/dT slope in comparison with the abrupt bending in the dehydration curve of the 19 Å to 15 Å states. This difference is probably related to the different temperature range of dehydration of the 19 Å to 15 Å states and the 15 Å to 12.5 Å states. The former crosses the L-V curve, whereas the latter occurs at temperatures above the critical point. The abrupt change in slope of the 19 Å to 15 Å dehydration boundary reflects the large density difference of the external H_2O on both sides of the L-V curve. For the 15 Å to 12.5 Å dehydration, the transition temperature is above the critical point of H_2O, thus the H_2O released by dehydration is in the supercritical vapor state. Because the density of the external H_2O increases gradually with increasing pressure and temperature in the supercritical state, the slope of the dehydration curve also increases gradually in this *P-T* regime.

Pressure dependence of rehydration hysteresis

Our data show that although pressure above the H_2O L-V curve does not have much effect on dehydration temperature, it has a pronounced effect on the rehydration hysteresis. Hysteresis clearly increases as pressure increases for both CaSWy-1 and MgSWy-1 (Figs. 7 and 9a). This suggests that pressure inhibits the rehydration process.

We suggest a hypothetical rehydration mechanism consisting of two stages. First, the montmorillonite in the hydration state with the smaller d value swells as interlayer H_2O molecules rearrange themselves. Second, H_2O molecules diffuse into the enlarged interlayer space. The opening up of the interlayer during the first stage is a process with a positive ΔV. This positive ΔV requires extra activation energy when the sample is under pressure, thus resulting in a pressure-induced hysteresis.

Homogeneous dehydration and interstratification

It is well known that the 001 peak broadening during a smectite hydration or dehydration is due to the interstratification of layers of different thicknesses or hydration states (e.g., Hendricks et al. 1940). Our peak-width analysis revealed that in the dehydration and rehydration processes between the 19 Å and 15 Å states, there are two distinct stages, homogeneous dehydration (between 19

and ~17.5 Å) and interstratification (between ~17.5 and 15 Å) (Figs. 4 and 5) This observation may aid in the understanding of the properties of interlayer H_2O molecules.

For all runs starting from the 19 Å hydration state, the 001 peak remained sharp as the basal spacing gradually decreased to ~17.5 Å. When the basal spacing dropped from ~17.5 to 15 Å, the 001 peak first broadened and then narrowed. If peak broadening is due to interstratification of the third and second hydration states, then the narrow peak width between 19 and ~17.5 Å indicates that the sample is in a homogeneous state, i.e., the d values of all layers are nearly identical. Several hypotheses to explain the hydration state between 19 and ~17.5 Å are discussed below.

One possibility is that the ~1.5 Å decrease in the d_{001} value in this range is due to compression of the (001) planes as pressure increases from room temperature to ~300 °C. Comparison of the P-T paths in Figure 2 and the data in Figure 4 suggests two problems with this interpretation. The first can be seen by following the pressure evolution of the heating path along the 0.877 g/cm^3 isochore; the pressure started to increase steeply at $T_h \approx$ 190 °C. The rate of change of d value before and after this temperature should be very different if the shrinking is due to compression; this was not observed (Fig. 4b). The second problem involves variations in pressure evolution for different heating paths. Because the pressure evolution of each heating path is different, the variations in d_{001} values should display different slopes when plotted against temperature for different isochoric paths; this also was not observed in the data (Figs. 4a–4c).

An alternative hypothesis to explain the change in d values from 19 to 17.5 Å is that within this temperature range the interlayer gradually loses some H_2O homogeneously throughout all layers. McBride et al. (1975) suggested that the interlayer H_2O in the third hydration state is very dynamic, i.e., not fixed in any specific position. Such a structure may tolerate partial H_2O loss and a decrease in thickness by up to 1.5 Å without collapsing to a more compact hydration state.

The FWHM evolution during rehydration also shows an interstratification stage when the average basal spacing is between 15 and 17.5 Å and a homogeneous rehydration between 17.5 and 19 Å. This reveals that the interlayer H_2O molecules needed to support a 17.5 Å interlayer spacing are different from the interlayer H_2O molecules needed to expand the spacing from 17.5 to 19 Å. The latter may have thermodynamic properties closer to those of the external bulk water, and the former may be more structurally bonded.

Stability of multilayer hydrates: A comparison with results from thermodynamic modeling

Our results, for the first time, clearly show that the 19 Å hydrate is stable at high H_2O pressure above the H_2O L-V curve up to 200–385 °C, depending on the species of interlayer cations. The fact that our experimental data show both dehydration and rehydration, and well-characterized H_2O density before and after experiments, demonstrates that the third hydration state (with $d_{001} \approx$ 19 Å at room temperature and 1 atm) is an equilibrium state and should be considered in the thermodynamic properties of the smectite in general.

On the basis of a 1 bar pressure study by Keren and Shainberg (1975), Ransom and Helgeson (1994) did not consider any interlayer H_2O greater than two layers (15 Å) as an equilibrium state in their thermodynamic calculations because they assumed the thermodynamic properties of H_2O in higher hydrates are about the same as those of bulk water. Therefore, in thermodynamic calculations, any effect from this H_2O would cancel across the reaction. Ransom and Helgeson (1995) treated the 15 Å hydrate and anhydrate as end-members of a solid solution. They calculated the extent of a continuous dehydration from the 15 Å state as a function of pressure and temperature on the basis of the above assumptions. In Figure 8, their calculation (Ransom and Helgeson 1995) of the 50% dehydration contour line for Ca-end-member smectite is plotted with our 19 Å to 15 Å dehydration data for CaSWy-1 below 2 kbar. For comparison with the geologically relevant heating paths, two versions of geotherms estimated for the Tertiary sediments in the Gulf Coast of the United States used in Ransom and Helgeson (1995) are also included in Figure 8.

Figure 8 clearly shows that the thermodynamic calculation is very different from the experimental results. Because our results demonstrate both dehydration and rehydration processes and reveal the effect of pressure, it is clear that the stable phase at high pressure and low temperature is the 19 Å state. Our data also show that the pressure-induced hysteresis is even greater for the 12.5 Å to 15 Å rehydration; this may explain the lack of any rehydration signal in previous experimental data (Koster van Groos and Guggenheim 1987).

A comparison between the current experimental data and the calculated curve in Figure 8 shows that even for pressures just above the H_2O L-V curve, where rehydration hysteresis is nearly zero, the dehydration temperature is already ~100 °C higher than the calculated value for the 50% dehydration from a 15 Å hydrate (Ransom and Helgeson 1995). From our data for MgSWy-1 and previous low-pressure data, it can be shown that the 15 Å state is stable up to at least 500–600 °C, which is more than 300 °C higher than the calculated value of Ransom and Helgeson (1995). According to the geotherms, our data also predict that up to 1.5 kbar, the pressure corresponding to ~6.5 km depth in the Gulf Basin, the Ca-end-member smectite can still hold a large amount of H_2O in the third (19 Å) hydration state.

Our data suggest that a better thermodynamic solid-solution model for the clay hydrate is needed to describe the dehydration behavior at high H_2O pressures. Such a model would consider various hydration states with discrete structures of H_2O as intermediate stable phases be-

TABLE 2. Summary of dehydration temperatures for various interlayer cations

Cation	19 Å to 15 Å	15 Å to 12.5 Å
Na^+	330–385 °C	485–500 °C
Ca^{2+}	260–350 °C	—
Mg^{2+}	200–250 °C	590–605 °C

tween the end-members, a fully hydrated state and an anhydrous state.

The effect of interlayer cations

It is well known that the species of interlayer cations is an important factor controlling the swelling behavior of the clay (e.g., McBride 1994). The primary factors are the size and charge of the cation. Therefore, to understand the effect of cation species on dehydration and rehydration under high pressure, it is useful to compare the present study on Ca- and Mg-exchanged montmorillonite with our previous study on Na-exchanged montmorillonite (Huang et al. 1994). Huang et al. (1994) showed that NaSWy-1 dehydrates from the 19 Å to the 15 Å state at 330–385 °C along the ~0.80 g/cm³ isochore. In Table 2 the NaSWy-1 dehydration data are compared with the dehydration-temperature range for CaSWy-1 (260–350 °C) and MgSWy-1 (200–250 °C) obtained at H_2O densities from 0.7–1.05 g/cm³ (Table 2). Also given in Table 2 are the dehydration temperatures for the 15 Å to 12.5 Å states obtained for NaSWy-1 by Huang et al. (1994) and for MgSWy-1 in this study at pressures above the H_2O L-V curve.

The ratio of charge to ionic radius (ionic potential) vs. the dehydration temperature is plotted in Figure 10 for Mg, Ca, and Na ions. It can be seen that the dehydration temperatures for the 19 Å to 15 Å conversion and for the 15 Å to 12.5 Å conversion have opposite trends. The former decreases with increasing ionic potential, whereas the later increases. The different trends may be explained by intermolecular forces.

The long-range electrostatic attractive force between the negatively charged silicate sheets and the positively charged cations is the dominant force binding the layers together. The cations, in addition to providing the cohesive force, affect the configuration of the interlayer H_2O molecules. The Mg ion, which is smaller than the Ca ion and has a higher charge than the Na ion, more strongly favors the sixfold coordination of H_2O molecules, much as it favors sixfold coordination in most oxides and silicates. The 15 Å hydrate owes its spacing to the sixfold coordination group. It seems reasonable, therefore, that the Mg-exchanged montmorillonite should have a 15 Å hydrate that is stable over a larger temperature range than those of the Ca- and Na-exchanged montmorillonite, as seen in Table 2 and Figure 10.

Other geophysical implications

The fact that the 19 Å hydrate is stable up to 200–380 °C under pressures along the geotherm is important for

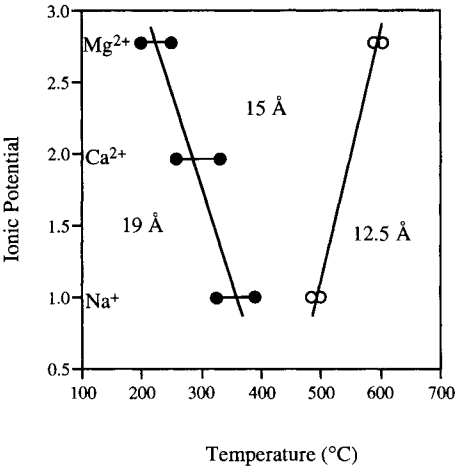

FIGURE 10. Ionic potentials (charge/radius) of Na^+, Ca^{2+}, and Mg^{2+} cations vs. dehydration temperature for SWy-1 montmorillonite exchanged with those cations. Pairs of connected dots represent the range over which dehydration occurs.

modeling of sedimentary basins and petroleum generation. In a sedimentary basin with K and other ions available, there is likely to be chemical alteration that would convert montmorillonite to illite and release H_2O during the reaction. This reaction is usually kinetically favorable below 200 °C. Most investigators have assumed that when clay releases H_2O during chemical alteration, there are only two layers of H_2O being released. Our results indicate that for any H_2O-releasing reaction occurring at <5 km, the 19 Å hydrate can release much more H_2O. The amount of H_2O released during those alteration processes is a crucial factor in attempts to model the subsurface hydrodynamics such as fluid migration in porous layers and overpressure build-up in closed water compartments.

Our results also indicate that clays in the 15 Å hydration state are stable up to 450–600 °C at pressures above the H_2O L-V curve. If the environment is relatively free of ions that might result in chemical alteration of montmorillonite, it can be transported down the subduction zone before H_2O is released. Dehydration in subduction zones is considered to be an important factor in causing shallow earthquakes. The H_2O released in the dehydration process in subduction zones also causes partial melting in the overlying mantle, and those melts are the source of igneous intrusions and volcanic activity along the plate boundaries.

Smectite clays are very ductile in comparison with their alteration products (Wang et al. 1980). If they can escape chemical alteration, our results show that those clays are stable to considerable crustal depths, where they may be the best candidates to form good seals for deep oil reservoirs.

REFERENCES CITED

Bassett, W.A., Shen, A.H., Bucknum, M.J., and Chou, I.-M. (1993) A new diamond anvil cell for hydrothermal studies to 2.5 GPa and from −190 to 1200 °C. Review of Scientific Instruments, 64, 2340–2345.

Burst, J.F. (1969) Diagenesis of Gulf Coast clayey sediments and its possible relation to petroleum migration. American Association of Petroleum Geologists Bulletin, 53, 73–93.

Chang, F.R.C., Skipper, N.T., Sposito, G. (1995) Computer simulation of interlayer molecular structure in sodium montmorillonite hydrates. American Chemical Society, 11, 2734–2741.

Clementz, D.M., Pinnavaia, T.J., and Mortland, M.M. (1973) Stereochemistry of hydrated copper(II) ions on the interlamellar surfaces of layer silicates. An electron spin resonance study. Journal of Physical Chemistry, 77, 196–200.

Hendricks, S.B., Nelson, R.A., and Alexander, L.T. (1940) Hydration mechanism of the clay mineral montmorillonite saturated with various cations. Journal of the American Chemical Society, 62, 1457–1464.

Hower, J.E., Hower, M.E., and Perry, E.A. (1976) Mechanism of burial metamorphism of argillaceous sediments: I. Mineralogical and chemical evidence. Geological Society of America Bulletin, 87, 725–737.

Huang, W.-L., Bassett, W.A., and Wu, T.C. (1994) Dehydration and hydration of montmorillonite at elevated temperatures and pressures monitored using synchrotron radiation. American Mineralogist, 79, 683–691.

Keren, R., and Shainberg, I. (1975) Water vapor isotherms and heat of immersion of Na/Ca-montmorillonite system: I. Homoionic clay. Clays and Clay Minerals, 23, 193–200.

Koster van Groos, A.F., and Guggenheim, S. (1984) The effect of pressure on the dehydration reaction of interlayer water in Na-montmorillonite (SWy-1). American Mineralogist, 69, 872–879.

———(1986) Dehydration of a K-exchanged montmorillonite (SWy-1) at elevated pressure. Clays and Clay Minerals, 34, 281–286.

———(1987) Dehydration of a Ca- and Mg-exchanged montmorillonite (SWy-1) at elevated pressures. American Mineralogist, 72, 292–298.

McBride, M.B. (1994) Environmental chemistry of soils, 406 p., Oxford, New York.

McBride, M.B., Pinnavaia, T.J., and Mortland, M.M. (1975) Electron spin resonance studies of cation orientation in restricted water layers on phyllosilicate (smectite) surfaces. Journal of Physical Chemistry, 79, 2430–2435.

McEwan, D.M.C., and Wilson, M.J. (1980) Interlayer and intercalation complexes of clay minerals. In G.W. Brindley and G. Brown, Eds., Clay structures of clay minerals and their X-ray diffraction, p. 197–248. Mineralogical Society, London.

Ransom, B., and Helgeson, H. (1994) A chemical and thermodynamic model of dioctahedral 2:1 layer clay minerals in diagenetic processes: Regular solution representation of interlayer dehydration in smectite. American Journal of Science, 294, 449–484.

———(1995) A chemical and thermodynamic model of dioctahedral 2:1 layer clay minerals in diagenetic processes: Dehydration of dioctahedral aluminous smectite as a function of temperature and depth in sedimentary basin. American Journal of Science, 295, 245–281.

Saul, A., and Wagner, W. (1989) A fundamental equation for water covering the range from the melting line to 1237K at pressure up to 25000 MPa. Journal of Physical and Chemical Reference Data, 18, 1537–1564.

Stone, R.L., and Rowland, R.A. (1955) DTA of kaolinite and montmorillonite under H_2O vapor pressure up to six atmospheres. Third National Conference of Clay Minerals Society, Houston, Texas, NAS-NRC, 39, 103–116.

Wagner, W., and Pruss, A. (1993) International equations for the saturation properties of ordinary water substance. Revised according to the international temperature scale of 1990. Addendum to Journal of Physical and Chemical Reference Data 16, 893 (1987). Journal of Physical and Chemical Reference Data, 22, 783–787.

Wagner, W., Saul, A., and Pruss, A. (1994) International equation for the pressure along the melting and the sublimation of ordinary water substance. Journal of Physical and Chemical Reference Data, 23, 515–527.

Wang, C.-Y., Mao, N.-S., and Wu, F.T. (1980) Mechanical properties of clays at high pressure. Journal of Geophysical Research, 85, 1462–1468.

Wu, T.-C., Shen, A.H., Weathers, M.S., Bassett, W.A., and Chou, I.-M. (1995) Anisotropic thermal expansion of calcite at high pressures: An in situ X-ray diffraction study in a hydrothermal diamond-anvil cell. American Mineralogist, 80, 941–946.

Manuscript received September 18, 1995
Manuscript accepted October 17, 1996